SPARSE MMSE EQUALIZER FOR GTR-STBC IN AERONAUTICAL TELEMETRY

Md. Shah Afran
Mohammad Saquib
The University of Texas at Dallas

Michael Rice
Brigham Young University

ABSTRACT

This paper investigates the performance of sparse minimum mean squared error (MMSE) equalizer for generalized time-reversed space-time block codes (GTR-STBC) in aeronautical telemetry. GTR-STBC equipped with MMSE equalizer performs the best trade-off between the signal-to-noise ratio and inter-symbol interference by allocating unequal power over aeronautical telemetry channels. However, aeronautical telemetry channels are in general consists of larger delay spreads which make the MMSE equalization of aeronautical channels with GTR-STBC computationally complex. Interestingly enough, in spite of larger delays aeronautical channels are made of few sparsely distributed multipaths and therefore their MMSE equalizers are highly compressible. In this paper, compressed sensing based greedy algorithm is used for the design of sparse MMSE equalizer and a convex curve-fitting algorithm is used to find the sub-optimum power allocation parameter at the same sparsity level for GTR-STBC. Our simulation results show that 75-90% of the non-zero equalizer taps can be reduced with a slight relaxation of the mean-squared error (or equivalently slight degradation of bit-error rate performance). It is also observed that the optimum transmitter power profile for the sparse MMSE equalizer is different than that of the non-sparse equalizer.

INTRODUCTION

Aeronautical telemetry deals with a wideband air-to-ground communication link that usually comprises of frequency selective fading channels. In addition, severe size, weight and power limitations are imposed on the airborne transmitter. Highly power-efficient transmitters, such as radio frequency (RF) power amplifiers operating in full saturation, and constant-envelope modulation schemes are employed to overcome these limitations. Since frequency selective fading leads to inter-symbol interference (ISI), techniques for mitigating ISI using the aeronautical telemetry standard IRIG 106 [1] [especially the shaped offset quaternary phase shift keying version TG

(SOQPSK-TG)] are of immediate interest. The goal therefore is one involving single-carrier, constant-envelope modulation operating in a frequency selective channel. This is clearly an equalization and/or diversity problem. Diversity reception, especially by widely separated antennas, is an obvious but expensive solution. Another feasible solution is transmit diversity when the size, weight and power constraints allow it. The most common scenario will be a system involving multiple transmit antennas with a single receive antenna, which can increase the reliability or throughput in multipath fading channels.

Generalized time-reversed space-time block codes (GTR-STBC), which is a modified version of TR-STBC and incorporates the unequal power allocation ρ, is introduced in [2]. Because TR-STBC and its generalized version involve the combination of diversity processing and equalization, a suitable minimum mean squared error (MMSE) equalization technique for SOQPSK-TG was also designed in [2]. Equipped with GTR-STBC and a suitable equalization technique, post-equalizer mean-squared error was used to identify the optimum ρ. The conceptual tool of unequal power allocation together with GTR-STBC is used as a simple transmit diversity scheme based on the partial knowledge of the channel by the transmitter. Here, the transmitter only needs to know ρ, which is easy to compute at the receiver and send back to the transmitter. This simple scheme includes transmit selection diversity ($\rho = 0$ or 1) and traditional TR-STBC ($\rho = {}^1\!/_2$), and therefore, performs better than both of them.

Number of equalizer taps grows proportionally to the product of the number of input and output antennas for multiple-input multiple-output (MIMO) systems [3, 4]. Therefore, sparse equalizers will be crucial for GTR-STBC to reduce the computational complexity of equalization which is proportional to the number of non-zero equalizer taps. Sparse equalizers also offer other benefits over their non-sparse counterpart. As the number of non-zero taps is small, a sparse equalizer can adapt rapidly to changing channel conditions and can support systems with high mobility. Sparse equalizer can even perform better than non-sparse equalizer under non-ideal channel estimation. In [5], it was shown that more than 50% of the non-sparse equalizer taps has a very small contribution to the equalizer output signal-to-noise ratio (SNR). These filter taps which would be almost zero for ideal case contribute mostly noise in non-ideal channel estimation case. As a result, elimination of these taps could lead to performance improvement of the equalization.

In this paper, we explore compressed sensing based sparse equalization in the context of GTR-STBC. A joint optimization problem is designed to calculate the sparse GTR-STBC equalizer coefficients and unequal power allocation parameter ρ. The criterion for selecting the optimum ρ for sparse equalizer is to minimize the non-zero support of equalizer and also the post-equalizer mean-squared error (MSE) simultaneously given a maximum allowable loss in MSE. This behavior is illustrated in Figure 1, from which, we can also conclude that this joint optimization problem is mathematically untractable (MSE curves are in general non-convex). Therefore, we take a sub-optimum approach where we use a convex curve fitting method to calculate the sparse equalizer and also the power allocation parameter ρ for sparse GTR-STBC equalization.

Our numerical results show that a significant reduction in number of active taps can be achieved with a slight relaxation of the mean-squared error (or equivalently slight degradation of bit-error rate performance). The optimum transmitter power profile for the sparse MMSE equalizer is also observed to be different than that of the non-sparse equalizer.

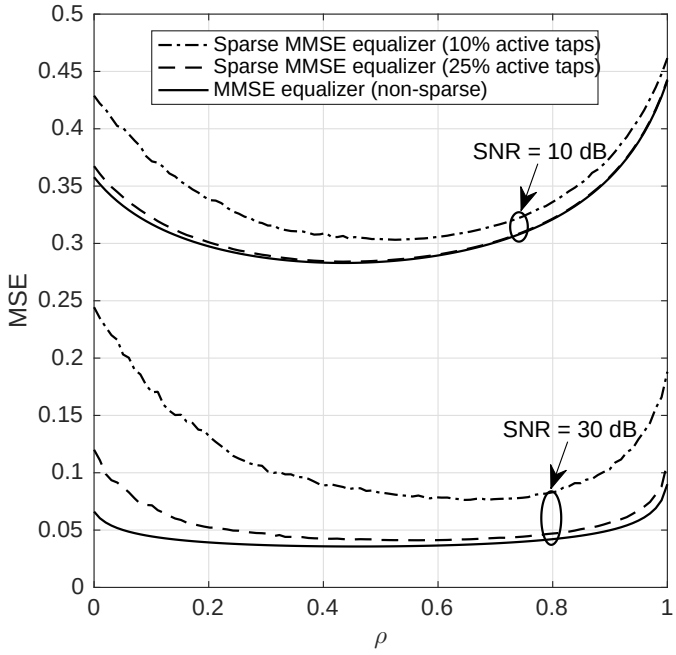

Figure 1: Plot of MSE vs power allocation parameter for GTR-STBC with both sparse and non-sparse MMSE equalizers. A pair of measured channel impulse responses from Cairns Army Airfield, Ft. Rucker, Alabama were used.

SPARSE MMSE EQUALIZATION OF SOQPSK-TG

The system considered here is summarized in Figure 2. As before, the complex-valued baseband equivalent representation [6] is used for all signals. Starting with the block diagram of Figure 2 (a), the SOQPSK-TG signal $x_c(t)$ is transmitted through a channel impulse response $h_c(t)$ whose output, accompanied by thermal noise, forms the receive signal $r_c(t)$. After the application of an anti-aliasing low-pass filter with impulse response $h_a(t)$, T-spaced samples of $r_c(t)$ are produced by an A/D converter. Assuming the anti-aliasing filter does not distort the received signal, the samples of the received signal may be expressed as

$$r(n) = x(n) * h(n) + w(n) = \sum_{k=-L_1}^{L_2} h(k)x(n-k) + w(n), \tag{1}$$

where

$$r(n) = r_c(nT), \qquad x(n) = x_c(nT), \qquad h(n) = \left. h_c(t) * h_a(t) \right|_{t=nT}.$$

In (1) $w(n)$ is the n-th sample of a zero-mean complex-valued Gaussian random sequence with autocorrelation function

$$R_w(k) = \frac{1}{2}\mathrm{E}\left\{w(n)w^*(n-k)\right\} = \sigma_w^2\delta(k). \tag{2}$$

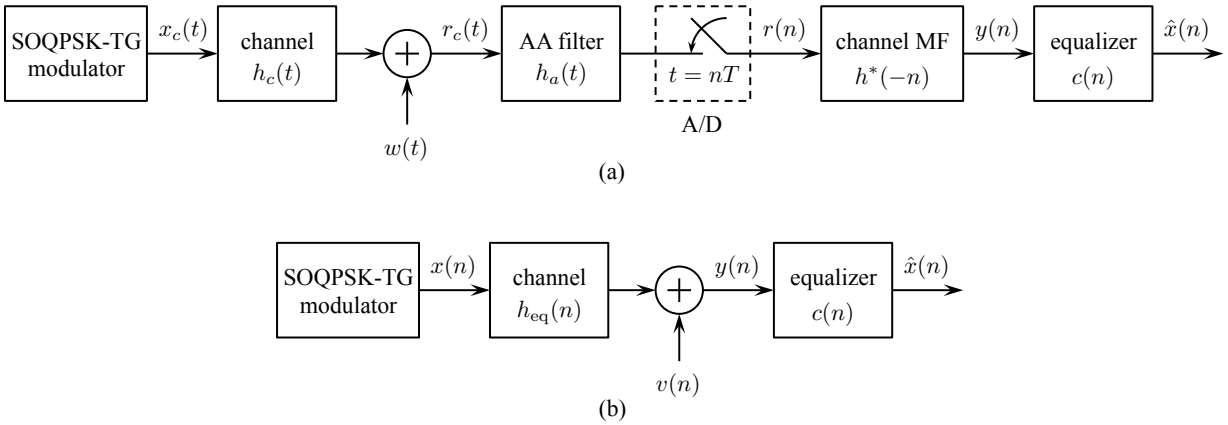

Figure 2: A block diagram of the system that applies an MMSE equalizer to samples of a received SOQPSK-TG signal: (a) the system showing the continuous-time signals, the anti-aliasing filter, and A/D converter; (b) the equivalent discrete-time system.

Note that (1) assumes the discrete-time channel has support on $-L_1 \leq n \leq L_2$. As a first step, we apply the samples $r(n)$ to a filter matched to the discrete-time channel to produce $y(n)$:

$$\begin{aligned} y(n) &= r(n) * h^*(-n) \\ &= x(n) * \underbrace{h(n) * h^*(-n)}_{h_{\text{eq}}(n)} + \underbrace{w(n) * h^*(-n)}_{v(n)} \qquad (3) \\ &= \sum_{k=-L_{\text{eq}}}^{L_{\text{eq}}} h_{\text{eq}}(k) x(n-k) + v(n), \qquad (4) \end{aligned}$$

where $L_{\text{eq}} = L_1 + L_2$ and $v(n)$ is a complex valued Gaussian random sequence with zero mean and autocorrelation function

$$R_v(k) = \frac{1}{2}\text{E}\left\{v(n)v^*(n-k)\right\} = \sigma_w^2 h_{\text{eq}}(k). \qquad (5)$$

The samples $y(n)$ form the input to an MMSE equalizer. The MMSE equalizer is an FIR filter with coefficients $c(n)$ for $-L_c \leq n \leq L_c$ designed to minimize the mean squared error between the equalizer filter output $\hat{x}(n)$ and the sequence $x(n)$. The entire system may be represented by an equivalent discrete-time system shown in Figure 2 (b).

Following the development in [2], the relationship between $x(n)$ and the equalizer output $\hat{x}(n)$ is

$$\hat{x}(n) = c(n) * y(n) = \sum_{k=-L_c}^{L_c} c(k) y(n-k). \qquad (6)$$

The vector of filter coefficients that minimizes the mean squared error

$$\mathcal{E} = \text{E}\left\{\left|x(n) - \hat{x}(n)\right|^2\right\}, \qquad (7)$$

is given by [2]

$$\mathbf{c} = \left[\mathbf{G}\mathbf{G}^{\dagger} + \frac{2}{E_b/N_0}\mathbf{H}_{\text{eq}}\right]^{-1}\mathbf{g}^{\dagger}, \tag{8}$$

where $\mathbf{c}$ is the $(2L_c+1)\times 1$ vector of filter coefficients, $\mathbf{G}$ is the $(2L_c+1)\times(2L_c+1+2L_{\text{eq}})$ matrix

$$\mathbf{G} = \begin{bmatrix} h_{\text{eq}}(L_{\text{eq}}) & \cdots & h_{\text{eq}}(-L_{\text{eq}}) & & \\ & h_{\text{eq}}(L_{\text{eq}}) & \cdots & h_{\text{eq}}(-L_{\text{eq}}) & \\ & & \ddots & & \\ & & & h_{\text{eq}}(L_{\text{eq}}) & \cdots \quad h_{\text{eq}}(-L_{\text{eq}}) \end{bmatrix}; \tag{9}$$

$\mathbf{H}_{\text{eq}}$ is the $(2L_c+1)\times(2L_c+1)$ matrix given by

$$\mathbf{H}_{\text{eq}} = \begin{bmatrix} h_{\text{eq}}(0) & \cdots & h_{\text{eq}}(-2L_c) \\ \vdots & & \vdots \\ h_{\text{eq}}(2L_c) & \cdots & h_{\text{eq}}(0) \end{bmatrix}, \tag{10}$$

where it is understood that $h_{\text{eq}}(k) = 0$ for $|k| > L_{\text{eq}}$.

Vector $\mathbf{g}$ is the $1\times(2L_c+1)$ vector given by

$$\mathbf{g} = \begin{bmatrix}\mathbf{0}_{1\times(L_c-L_{\text{eq}})} & \mathbf{h}_{\text{eq}} & \mathbf{0}_{1\times(L_c-L_{\text{eq}})}\end{bmatrix}, \tag{11}$$

where $\mathbf{0}_{1\times(L_c-L_{\text{eq}})}$ is a row vector comprising $L_c - L_{\text{eq}}$ zeros (here we assume $L_c > L_{\text{eq}}$, i.e., the equalizer is longer than the channel), and $\mathbf{h}_{\text{eq}}$ is the $1\times(2L_{\text{eq}}+1)$ vector given by

$$\mathbf{h}_{\text{eq}} = \begin{bmatrix} h_{\text{eq}}(L_{\text{eq}}) & \cdots & h_{\text{eq}}(0) & \cdots & h_{\text{eq}}(-L_{\text{eq}}) \end{bmatrix}. \tag{12}$$

The corresponding mean squared error is

$$\mathcal{E}_{\text{min}} = \sigma_x^2\left(1 - \mathbf{g}\left[\mathbf{G}\mathbf{G}^{\dagger} + \frac{2}{E_b/N_0}\mathbf{H}_{\text{eq}}\right]^{-1}\mathbf{g}^{\dagger}\right). \tag{13}$$

Now for the design of sparse equalizer from (7), at first we write $\mathcal{E}$ as a functions of $\mathbf{c}_{\text{s}}$. Putting $\left[\mathbf{G}\mathbf{G}^{\dagger} + \frac{2}{E_b/N_0}\mathbf{H}_{\text{eq}}\right] = \mathbf{M}$ we can write [4]

$$\mathcal{E}(\mathbf{c}_{\text{s}}) = \sigma_x^2\left(\underbrace{1 - \mathbf{g}\mathbf{M}^{-1}\mathbf{g}^{\dagger}}_{\mathcal{E}_{\text{min}}/\sigma_x^2} + \underbrace{(\mathbf{c}_{\text{s}} - \mathbf{c})\mathbf{M}(\mathbf{c}_{\text{s}} - \mathbf{c})^{\dagger}}_{\mathcal{E}_{\text{ex}}}\right). \tag{14}$$

Here, $\mathbf{c} = \mathbf{M}^{-1}\mathbf{g}^{\dagger}$ and $\mathcal{E}_{\text{ex}}$ is the term which represents the increase in normalized mean squared error due to the sparse equalizer $\mathbf{c}_{\text{s}}$. This term is equal to zero when we use equalizer $\mathbf{c}$ instead, but MMSE equalizer is generally non-sparse. Therefore, we allow a tradeoff between performance and complexity by $\mathcal{E}_{\text{ex}}$. Interestingly enough, results from sparse equalization literature ([4] and

references therein) show that, in general a slight relaxation of $\mathcal{E}$ through $\mathcal{E}_{\text{ex}}$ can achieve highly sparse filters. Using either Cholesky factorization or eigen decomposition of matrix $\mathbf{M}$, we can write $\mathbf{M} = \mathbf{M}_1\mathbf{M}_1^\dagger$, which formulates our sparse equalizer design problem as

$$\hat{\mathbf{c}}_{\text{s}} = \underset{\mathbf{c}_{\text{s}} \in \mathbb{C}^{2L_c+1}}{\operatorname{argmin}} \|\mathbf{c}_{\text{s}}\|_0 \quad \text{subject to} \quad \|\mathbf{M}_1^\dagger(\mathbf{c}_{\text{s}} - \mathbf{c})\|_2^2 \leq \epsilon, \tag{15}$$

where $\|\mathbf{M}_1^\dagger(\mathbf{c}_{\text{s}} - \mathbf{c})\|_2^2 = \mathcal{E}_{\text{ex}}$ and $\epsilon > 0$ is a design parameter which amounts the relaxation in MSE for the design of sparse filter. Here $\|\mathbf{c}_{\text{s}}\|_0$ is used to denote the number of nonzero entries of $\mathbf{c}_{\text{s}}$ while $\|\cdot\|_2^2$ denotes square of l_2 norm of a vector. However, in general, the optimal design of sparse filter is NP-hard [7]. Therefore, we will use sub-optimum algorithms described in [4]. In this paper, we use orthogonal matching pursuit (OMP) algorithm for sparse equalizer design as it gives us better control on calculating nonzero taps [8]. We denote the OMP operation by $\hat{\mathbf{c}}_{\text{s}} = \text{OMP}(\mathbf{b}, \mathbf{A}, \text{stopping criterion})$, where $\mathbf{b}$ is a known data vector and $\mathbf{A}$ denotes the sensing matrix. OMP is a greedy algorithm which tries to iteratively select a set of columns from $\mathbf{A}$ that are most correlated with $\mathbf{b}$ and then it solves a restricted least-squares problem using the selected columns. The stopping criterion can be a predefined sparsity level (number of nonzero entries) of $\hat{\mathbf{c}}_{\text{s}}$ or the upper-bound on loss in MSE (ϵ). In our numerical study we will use the first criterion. Using either $\mathbf{M} = \mathbf{M}_1\mathbf{M}_1^\dagger$ (Cholesky factorization) or $\mathbf{M} = \mathbf{U}\mathbf{\Lambda}\mathbf{U}^\dagger$ (eigen decomposition) with $\mathbf{c} = \mathbf{M}^{-1}\mathbf{g}^\dagger$ in (15), we can make following call to the OMP algorithm for the calculation of $\mathbf{c}_{\text{s}}$

$$\hat{\mathbf{c}}_{\text{s}} = \text{OMP}\left(\mathbf{M}_1^{-1}\mathbf{g}^\dagger, \mathbf{M}_1^\dagger, \|\hat{\mathbf{c}}_{\text{s}}\|_0 = k\right). \tag{16}$$

SPARSE MMSE EQUALIZATION FOR GENERALIZED TR-STBC (GTR-STBC)

An abstraction (to the sample level) for a 2×1 TR-STBC system is illustrated in Figure 3. Here the system transmits $2L$ samples of an SOQPSK-TG signal sampled at N samples/bit over two transmit antennas to one receive antenna. The equivalent discrete-time channel between transmit antenna 1 and the receive antenna is represented by the impulse response $h_1(n)$ for $-L_{1,1} \leq n \leq L_{1,2}$ whereas the equivalent discrete-time channel between transmit antenna 2 and the receive antenna is represented by the impulse response $h_2(n)$ for $-L_{2,1} \leq n \leq L_{2,2}$.

The TR-STBC encoder partitions the sample sequence $x(0), \ldots, x(2L-1)$ into two sequences $x_1(n)$ and $x_2(n)$ as shown in Figure 3. The length-$2L$ packet is transmitted in two intervals[1] each spanning L sample intervals. During the first interval $x_1(0), \ldots, x_1(L-1)$ is transmitted from antenna 1 whereas $x_2(0), \ldots, x_2(L-1)$ is transmitted from antenna 2. During the second interval, $x_2^*(L-1), \ldots, x_2^*(0)$ is transmitted from antenna 1 whereas $-x_1^*(L-1), \ldots, -x_1^*(0)$ is transmitted from antenna 2.

Power division using $0 \leq \rho \leq 1$ is accomplished by modified the TR-STBC system along the lines illustrated in Figure 3. Amplitude scaling is applied to the signals entering each channel so as to divide the power between the channels. Here ρ represents the proportion of total power allocated

[1] In a practical implementation, a guard interval at least as long as the longest channel impulse response must be inserted between the two intervals. Here, such an interval is assumed, although we won't complicate the notation to make this explicit.

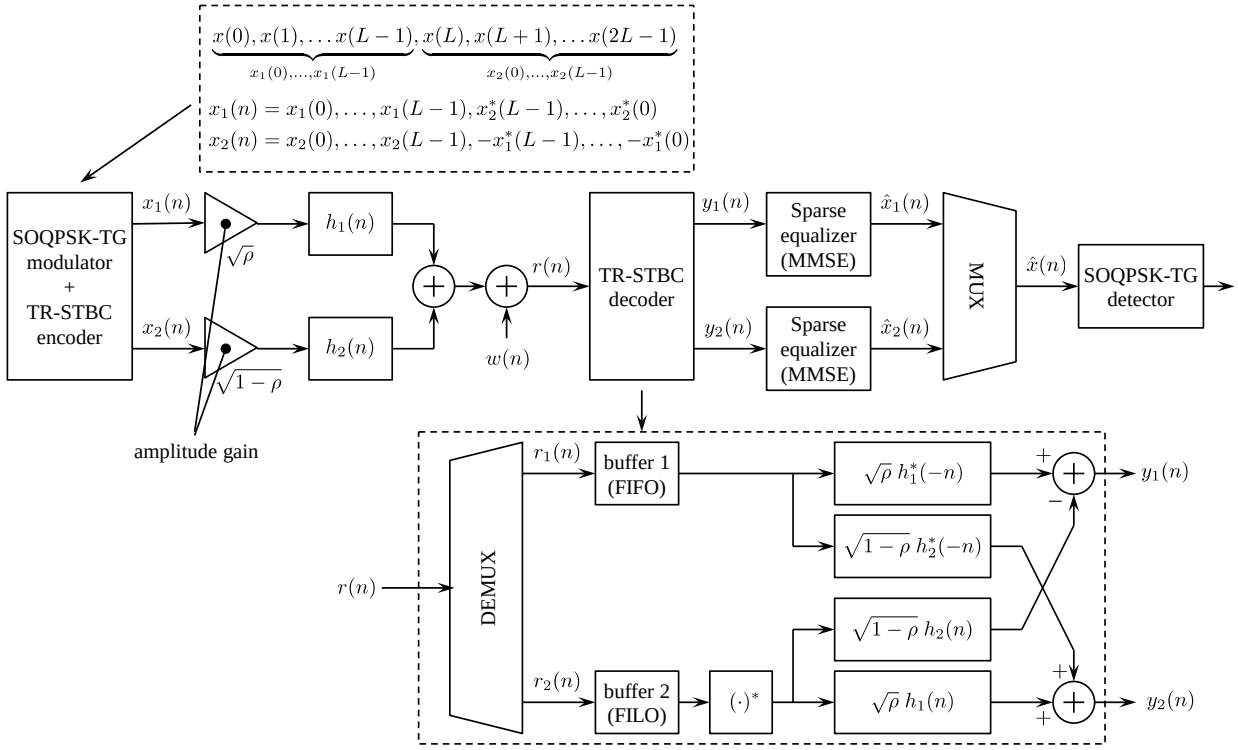

Figure 3: A block diagram of the TR-STBC system based on sparse equalizer and unequal power allocation using $0 \leq \rho \leq 1$.

to transmit antenna 1. The traditional TR-STBC system[2] is a special case for which $\rho = 1/2$. The square-root is used in Figure 3 because the amplitudes are what are being modified—the energy (or power) is the square of the amplitude.

The received signal $r(n)$ is given by

$$r(n) = \sqrt{\rho}\, x_1(n) * h_1(n) + \sqrt{1-\rho}\, x_2(n) * h_2(n) + w(n), \tag{17}$$

where $w(n)$ is a complex-valued Gaussian random sequence with zero mean and autocovariance function given by (2). The TR-STBC decoder partitions $r(n)$ into $r_1(n)$ and $r_2(n)$ as follows:

$$\begin{aligned} r_1(n) &= r(n) \text{ for } 0 \le n \le L-1 \\ r_2(n-L) &= r(n) \text{ for } L \le n \le 2L-1. \end{aligned} \tag{18}$$

These two sequences are given by

$$r_1(n) = \sqrt{\rho}\, x_1(n) * h_1(n) + \sqrt{1-\rho}\, x_2(n) * h_2(n) + w_1(n) \tag{19}$$

$$r_2(n) = \sqrt{\rho}\, x_2^*(-n) * h_1(n) - \sqrt{1-\rho}\, x_1^*(-n) * h_2(n) + w_2(n), \tag{20}$$

where $w_1(n)$ and $w_2(n)$ are related to $w(n)$ the same way $r_1(n)$ and $r_2(n)$ are related to $r(n)$. The TR-STBC decoder processes $r_1(n)$ and $r_2(n)$ using a bank of filters based on the channel impulse responses $h_1(n)$ and $h_2(n)$ as shown. The result of this processing is a pair of parallel sequences $y_1(n)$ and $y_2(n)$ which may be expressed as

$$\begin{aligned} y_1(n) &= r_1(n) * \sqrt{\rho}\, h_1^*(-n) - r_2^*(-n) * \sqrt{1-\rho}\, h_2(n) \\ &= x_1(n) * \underbrace{\Big[\rho\, h_1(n) * h_1^*(-n) + (1-\rho)\, h_2(n) * h_2^*(-n)\Big]}_{h_{\text{eq}}(n)} \\ &\qquad + \underbrace{w_1(n) * \sqrt{\rho}\, h_1^*(-n) + w_2^*(-n) * \sqrt{1-\rho}\, h_2(n)}_{v_1(n)}, \end{aligned} \tag{21}$$

and

$$\begin{aligned} y_2(n) &= r_1(n) * \sqrt{1-\rho}\, h_2^*(-n) + r_2^*(-n) * \sqrt{\rho}\, h_1(n) \\ &= x_2(n) * \underbrace{\Big[(1-\rho)\, h_2(n) * h_2^*(-n) + \rho\, h_1^*(-n) * h_1(n)\Big]}_{h_{\text{eq}}(n)} \\ &\qquad + \underbrace{\sqrt{1-\rho}\, w_1(n) * h_2^*(-n) + \sqrt{\rho}\, w_2^*(-n) * h_1(n)}_{v_2(n)}. \end{aligned} \tag{22}$$

These equations show that the equivalent composite channel for non-equal power allocation is

$$h_{\text{eq}}(n) = \rho\, \underbrace{h_1(n) * h_1^*(-n)}_{\eta_1(n)} + (1-\rho)\, \underbrace{h_2(n) * h_2^*(-n)}_{\eta_2(n)}. \tag{23}$$

[2]In the traditional TR-STBC system, $\rho = 1/2$ is included in neither the development nor the notation because the same power is assumed to be applied to each channel. Hence there is no need to account for it, other than in normalizing the noise variance.

Because the support for $h_1(n)$ is $-L_{1,1} \leq n \leq L_{1,2}$, the support for $\eta_1(n)$ is $-(L_{1,1}+L_{1,2}) \leq n \leq (L_{1,1}+L_{1,2})$. Similarly because the support for $h_2(n)$ is $-L_{2,1} \leq n \leq L_{2,2}$, the support for $\eta_2(n)$ is $-(L_{2,1}+L_{2,2}) \leq n \leq (L_{2,1}+L_{2,2})$. Consequently, the support for $h_{\text{eq}}(n)$ is $-L_{\text{eq}} \leq n \leq L_{\text{eq}}$ where

$$L_{\text{eq}} = \max\left\{L_{1,1}+L_{1,2}, L_{2,1}+L_{2,2}\right\}. \tag{24}$$

The noise sequences $v_1(n)$ and $v_2(n)$ are complex-valued Gaussian random sequences each with zero mean and autocorrelation and cross correlation functions

$$\frac{1}{2}\text{E}\left\{v_1(n)v_1^*(n-k)\right\} = \frac{1}{2}\text{E}\left\{v_2(n)v_2^*(n-k)\right\} = \sigma_w^2 h_{\text{eq}}(k). \tag{25}$$

$$\text{E}\left\{v_1(n)v_2^*(n-k)\right\} = 0. \tag{26}$$

By way of summary, the TR-STBC system presents to the equalizers the sequences $y_1(n)$ and $y_2(n)$ which may be represented by

$$y_1(n) = x_1(n) * h_{\text{eq}}(n) + v_1(n), \tag{27}$$
$$y_2(n) = x_2(n) * h_{\text{eq}}(n) + v_2(n), \tag{28}$$

where $h_{\text{eq}}(n)$ is given by (23). The noise terms $v_1(n)$ and $v_2(n)$ are uncorrelated zero-mean Gaussian random sequences each with autocorrelation function (25). A pair of equalizers operate in parallel on $y_1(n)$ and $y_2(n)$. Because the the noise sequences $v_1(n)$ and $v_2(n)$ are statistically equivalent and $h_{\text{eq}}(n)$ is common to both, the pair of equalizers operating on $y_1(n)$ and $y_2(n)$ are identical as long as $a_1(n)$ and $a_2(n)$ are statistically equivalent (the usual case). Any equalizer can be applied here (linear or non-linear, with or without noise whitening) with the usual performance-complexity tradeoffs. Here, we apply the approximate MMSE equalizer introduced in the previous section because the MMSE equalizer permit a mathematically tractable analysis for the resulting mean-squared error. We leverage the analytical expression to find the value of ρ that minimizes the mean squared error.

The equalizer filters of Figure 3 are identical, and the vector of filter coefficients is given by (8) and the corresponding mean squared error is given by (13). In these equations, $\mathbf{G}$, $\mathbf{g}$, and $\mathbf{H}_{\text{eq}}$ may be expressed in terms of power allocation parameter ρ. Using (23), it is straightforward to show that

$$\mathbf{G} = \rho\mathbf{G}_1 + (1-\rho)\mathbf{G}_2, \tag{29}$$
$$\mathbf{g} = \rho\mathbf{g}_1 + (1-\rho)\mathbf{g}_2, \tag{30}$$
$$\mathbf{H}_{\text{eq}} = \rho\mathbf{H}_1 + (1-\rho)\mathbf{H}_2, \tag{31}$$

where $\mathbf{G}_1$, $\mathbf{g}_1$, and $\mathbf{H}_1$ are formed from $\eta_1(n)$ the same way $\mathbf{G}$, $\mathbf{g}$, and $\mathbf{H}_{\text{eq}}$ are formed from $h_{\text{eq}}(n)$, respectively. Similar definitions apply to $\mathbf{G}_2$, $\mathbf{g}_2$, and $\mathbf{H}_2$ with $\eta_2(n)$. Making the substitutions for $\mathbf{G}(\rho)$, $\mathbf{g}(\rho)$, and $\mathbf{H}_{\text{eq}}(\rho)$ gives

$$\mathbf{c}(\rho) = \mathbf{M}(\rho)^{-1}\mathbf{g}(\rho)^\dagger, \tag{32}$$

and

$$\mathcal{E}_{\text{min}}(\rho) = \sigma_x^2\left[1 - \mathbf{g}(\rho)\mathbf{M}(\rho)^{-1}\mathbf{g}(\rho)^\dagger\right]. \tag{33}$$

Here $\mathbf{c}(\rho)$ is non-sparse MMSE equalizer and $\mathcal{E}_{\text{min}}(\rho)$ is the MSE, where

$$\mathbf{M}(\rho) = \left[\mathbf{G}(\rho)\mathbf{G}(\rho)^{\dagger} + \frac{2}{E_b/N_0}\mathbf{H}_{\text{eq}}(\rho)\right]. \tag{34}$$

Let $\rho_{\text{opt,ns}}$ is the optimum ρ for non-sparse equalizer which minimizes (33). Therefore, $\mathcal{E}_{\text{min}}(\rho_{\text{opt,ns}})$ is the minimum attainable MSE of the system with equalizer $\mathbf{c}(\rho_{\text{opt,ns}})$. Now, following the development in the previous section, for sparse GTR-STBC equalizer $\mathbf{c}_{\text{s}}(\rho)$, we can find MSE as a function of both ρ and $\mathbf{c}_{\text{s}}(\rho)$

$$\mathcal{E}(\rho, \mathbf{c}_{\text{s}}(\rho)) = \sigma_x^2\left[1 - \mathbf{g}(\rho)\mathbf{M}(\rho)^{-1}\mathbf{g}(\rho)^{\dagger} + \Big(\mathbf{c}_{\text{s}}(\rho) - \mathbf{c}(\rho)\Big)\mathbf{M}(\rho)\Big(\mathbf{c}_{\text{s}}(\rho) - \mathbf{c}(\rho)\Big)^{\dagger}\right], \tag{35}$$

where similar to (16) $\mathbf{c}_{\text{s}}(\rho)$ can be computed by following call to the OMP algorithm

$$\hat{\mathbf{c}}_{\text{s}}(\rho) = \text{OMP}\left(\mathbf{M}_1^{-1}(\rho)\mathbf{g}(\rho)^{\dagger}, \mathbf{M}_1^{\dagger}(\rho), \|\hat{\mathbf{c}}_{\text{s}}(\rho)\|_0 = k\right). \tag{36}$$

Since $\mathcal{E}_{\text{min}}(\rho_{\text{opt,ns}})$ is the minimum attainable MSE, the term $\mathcal{E}_{\text{excess}}$ which represents the increase of MSE for GTR-STBC in dB will be calculated as

$$\mathcal{E}_{\text{excess}}(\text{dB}) = 10\log_{10}\left(\frac{\mathcal{E}(\rho_{\text{opt}}, \mathbf{c}_{\text{s}}(\rho_{\text{opt}}))}{\mathcal{E}_{\text{min}}(\rho_{\text{opt,ns}})}\right). \tag{37}$$

However, unlike the MSE for non-sparse case as in (33), MSE for sparse equalization as given in (35) is mathematically untractable due to the non-convex nature of MSE function as shown in Figure 1. Therefore, finding the optimum ρ for sparse equalization is computationally challenging. As a result, we have taken a sub-optimum approach to calculate ρ_{opt} which will try to minimize $\mathcal{E}(\rho, \mathbf{c}_{\text{s}}(\rho))$. Our algorithm fits a convex curve after calculating $\mathcal{E}(\rho, \mathbf{c}_{\text{s}}(\rho))$ at few candidate values of ρ chosen from 0 to 1 with an interval of 0.25 (along with $\rho_{\text{opt,ns}}$). Later we use this convex curve to seek for lower MSE value.

NUMERICAL RESULTS

The forgoing analysis was applied to a helicopter-to-ground radio link using 1000 channel impulse responses from Cairn Army Airfield, Ft. Rucker, Alabama, captured during the channel sounding experiment described in [9]. For the modulation, we assume 10 Mbit/s SOQPSK-TG with the equalizers operating at 2 samples/bit. In the results shown below, $h_1(n)$ is the equivalent discrete-time channel between the nose antenna and the receive antenna and $h_2(n)$ is the channel between the tail antenna and the receive antenna.

Natural normalization is applied to the channels. Let $h_{1,\text{u}}(n)$ and $h_{2,\text{u}}(n)$ be unnormalized channel impulse responses for the two equivalent discrete-time channels obtained directly from the channel sounding data, and let

$$E_1 = \sum_{n=-L_{1,1}}^{L_{1,2}} |h_{1,\text{u}}(n)|^2; \qquad E_2 = \sum_{n=-L_{2,1}}^{L_{2,2}} |h_{2,\text{u}}(n)|^2, \tag{38}$$

be the energies in two channels. The natural normalization uses

$$h_1(n) = \frac{1}{\sqrt{E}} h_{1,\mathrm{u}}(n); \qquad h_2(n) = \frac{1}{\sqrt{E}} h_{2,\mathrm{u}}(n), \tag{39}$$

where $E = \max\{E_1, E_2\}$. This normalizes the stronger of the two channels to unit energy. We call this the natural normalization because in real multi-antenna scenarios, it is often the case that one of the channels is stronger than the other.

The numerical results were produced as follows. The values of ρ that minimize (33) and (35) for $L_c = 5 \times L_{\text{eq}}$ [10] were numerically computed for non-sparse and sparse equalizers, respectively. After that, (37) is used to calculate $\mathcal{E}_{\text{excess}}$ (dB). The corresponding results are shown in Figures 4 and 5, for $E_b/N_0 = 10$ dB and $E_b/N_0 = 16$ dB, respectively. Figure 4 shows that, at $E_b/N_0 = 10$ dB, a reduction of 75% equalizer taps is possible with a relaxation in MSE of < 0.06 dB. A relaxation in MSE of around 0.4 dB would allow us to eliminate more than 90% of the equalizer taps for the same E_b/N_0. However, for $E_b/N_0 = 16$ dB, Figure 5 indicates that more relaxation of MSE (more performance degradation) is required for similar sparsity levels. This is consistent with findings in [5], where it is shown that as E_b/N_0 increases the sparse equalizers need more active taps to maintain the similar performance in output SNR.

Figures 6 and 7 plots the optimum power profiles at $E_b/N_0 = 10$ dB and $E_b/N_0 = 16$ dB, respectively. We observe that the profile of ρ is different for sparse equalizers than the non-sparse MMSE equalizers. The profile of ρ for sparse equalizers also depend on the sparsity level (or equivalently on increase of MSE). Figure 1 explains this curious behaviour where it is observed that an increase of sparsity level changes the MSE curves along with the optimum choice of ρ.

In Figure 8, we compare the bit error rate (BER) of our proposed sparse MMSE equalizers with non-sparse MMSE equalizers for GTR-STBC. It is interesting to note from Figure 8 that at a 25% sparsity level both sparse and non-sparse equalizers have almost similar BER performances for E_b/N_0 of 10-12 dB. With a target BER of 10^{-4}, sparse equalizers with 25% active taps require only about 0.1 dB relaxation in E_b/N_0. For similar performance with a sparsity level of 10% about 1.5 dB relaxation is required.

CONCLUSIONS

In this paper, we investigated the performance of sparse MMSE equalizers for GTR-STBC using a set of measured channel impulse responses collected from helicopter-to-ground channel sounding experiments. Unlike the non-sparse case, sparse MMSE equalizers produce a non-convex MSE function which is mathematically untractable. Therefore, we proposed a convex curve-fitting based algorithm to find the ρ that sub-optimally minimizes MSE for sparse equalizers. Simulation results showed that at low to moderate SNR a huge reduction of non-zero equalizer taps can be achieved at the cost of a slight relaxation of MSE. It is also observed that depending on the system conditions the optimum value of ρ is very sensitive to the sparsity level of the equalizers.

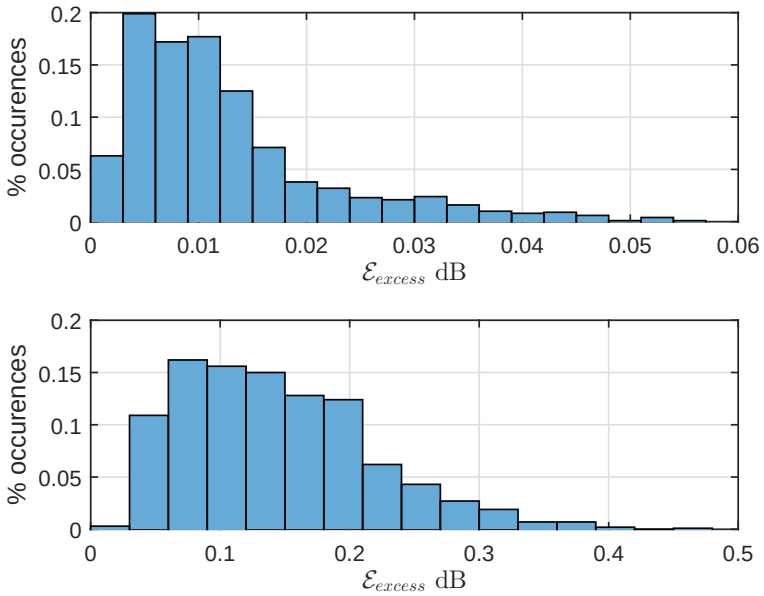

Figure 4: Increase of MSE with $E_b/N_0 = 10$ dB for 1000 pairs of measured channel impulse responses from Cairns Army Airfield, Ft. Rucker, Alabama: (top) sparse MMSE equalizer with 25% active taps; (bottom) sparse MMSE equalizer with 10% active taps.

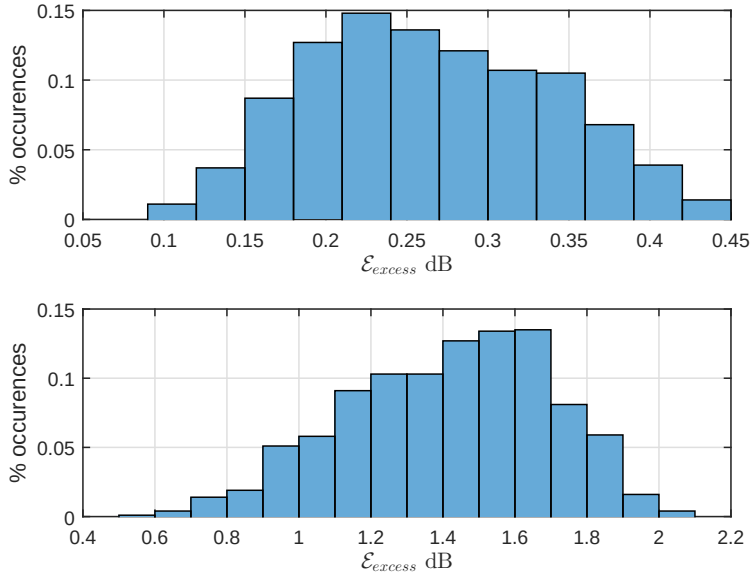

Figure 5: Increase of MSE with $E_b/N_0 = 16$ dB for 1000 pairs of measured channel impulse responses from Cairns Army Airfield, Ft. Rucker, Alabama: (top) sparse MMSE equalizer with 25% active taps; (bottom) sparse MMSE equalizer with 10% active taps.

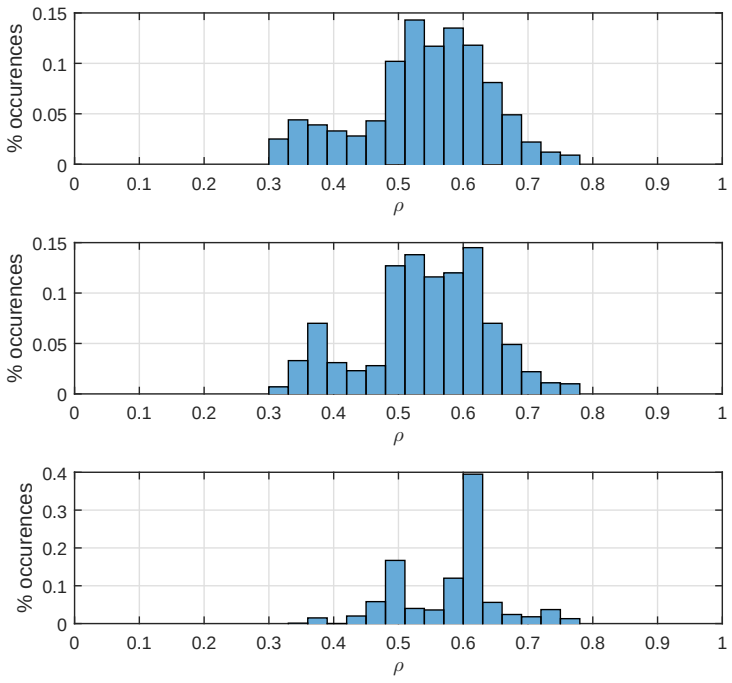

Figure 6: Optimum power allocations in the mean-squared error sense with $E_b/N_0 = 10$ dB for 1000 pairs of measured channel impulse responses from Cairns Army Airfield, Ft. Rucker, Alabama: (top) non-sparse MMSE equalizer; (middle) sparse MMSE equalizer with 25% active taps; (bottom) sparse MMSE equalizer with 10% active taps.

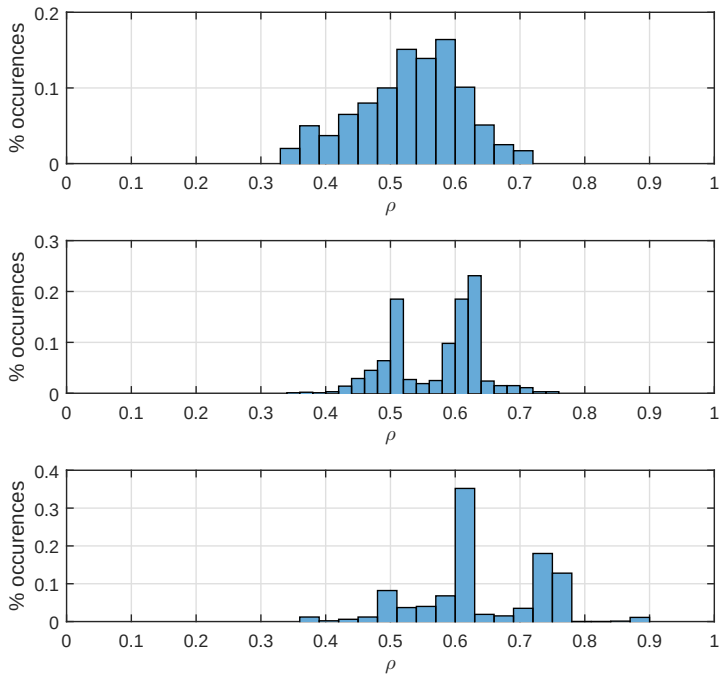

Figure 7: Optimum power allocations in the mean-squared error sense with $E_b/N_0 = 16$ dB for 1000 pairs of measured channel impulse responses from Cairns Army Airfield, Ft. Rucker, Alabama: (top) non-sparse MMSE equalizer; (middle) sparse MMSE equalizer with 25% active taps; (bottom) sparse MMSE equalizer with 10% active taps.

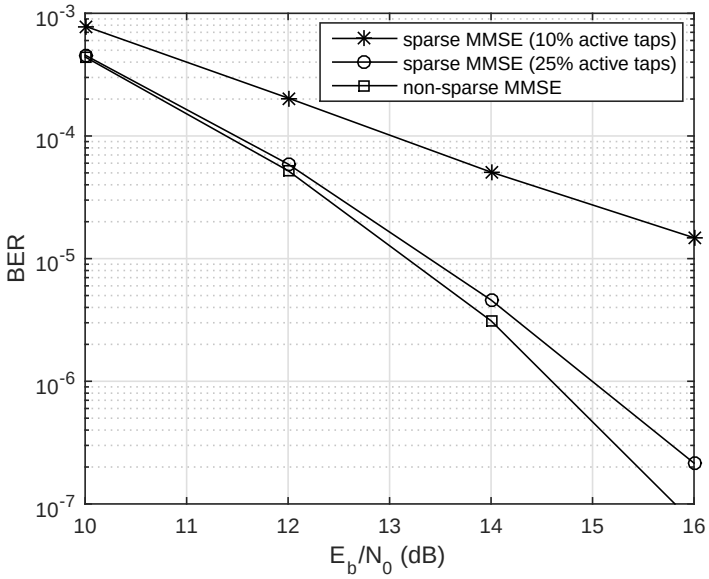

Figure 8: Comparison of average simulated BER for 1000 randomly selected channels from 39300 channel impulse responses measured at Cairns Army Airfield, Ft. Rucker, Alabama.

ACKNOWLEDGEMENTS

This project is funded by the Test Resource Management Center (TRMC) Test and Evaluation, Science & Technology (T&E/S&T) Program through the U.S. Army Program Executive Office for Simulation, Training, and Instrumentation (PEO STRI) under Contract No. W900KK-13-C-0026 (PAQ).

REFERENCES

[1] *IRIG Standard 106-04: Telemetry Standards*, Range Commanders Council Telemetry Group, Range Commanders Council, White Sands Missile Range, New Mexico, 2004, (Available on-line at http://www.wsmr.army.mil/RCCsite/Pages/Publications.aspx).

[2] M. Rice, M. Afran, and M. Saquib, "Equalization in aeronautical telemetry using multiple transmit antennas," *IEEE Transactions on Aerospace and Electronic Systems*, vol. 51, no. 5, pp. 2148 – 2165, jul 2015.

[3] D. Wei, C. Sestok, and A. Oppenheim, "Sparse filter design under a quadratic constraint: Low-complexity algorithms," *IEEE Transactions on Signal Processing*, vol. 61, no. 4, 2013.

[4] A. Gomaa and N. Al-Dhahir, "A new design framework for sparse FIR MIMO equalizers," *IEEE Transactions on Communications*, vol. 59, no. 8, 2011.

[5] G. Kutz and D. Raphaeli, "Determination of tap positions for sparse equalizers," *IEEE Transactions on Communications*, vol. 55, no. 9, 2007.

[6] J. Proakis and M. Salehi, *Digital Communications*, 5th ed. New York: McGraw-Hill, 2007.

[7] B. Natarajan, "Sparse approximate solutions to linear systems," *SIAM Journal on Computing*, vol. 24, 1995.

[8] J. Tropp and A. Gilbert, "Signal recovery from random measurements via orthogonal matching pursuit," *IEEE Transactions on Information Theory*, vol. 53, no. 12, pp. 4655–4666, 2007.

[9] M. Rice and M. Jensen, "Mulitpath propagation for helicopter-to-ground MIMO links," in *Proceedings of the IEEE Military Communications Conference*, Baltimore, MD, October 2011.

[10] J. Treichler, I. Fijalkow, and C. Johnson, "Fractionally spaced equalizers: How long should they be?" *IEEE Signal Processing Magazine*, May 1996.